

**APPENDIX 3.6.2
CALCULATION SUMMARY
INFILTRATION MODELING**

CALCULATION SUMMARY
APPENDIX 3.6.2
INFILTRATION MODELING

This modeling evaluation was undertaken to address comments regarding the adequacy of using a one-dimensional model to determine infiltration into the waste matrix. Models of the waste facilities have been developed using the USGS code VS2DI, Version 1.2 (Hsieh et al., 2000) to examine these issues. VS2DI is a graphical software package for simulating fluid flow and solute or energy transport in variably saturated porous media. Two types of models were developed using VS2DI: a two-dimensional (2-D) model for the CWF cover and one-dimensional (1-D) models for the waste areas of the FWF and CWF.

The 2-D model was developed to evaluate two-dimensional effects (such as bypass) on infiltration through the landfill cover. The 2-D model extends from the top of the sand lateral drainage layer (in the landfill) and the top of the OAG layer (in the undisturbed host medium) down to the elevation of the reinforced shotcrete header. Three scenarios were developed for the 2-D model assuming ⁽¹⁾ base case precipitation, ⁽²⁾ increased precipitation to represent a future wetter climate, and ⁽³⁾ base case precipitation with cover degradation.

To evaluate flow through the waste, 1-D models were developed for the FWF and CWF. These models extended from the base of the non-select red bed fill to the base of the waste site. Flow rates for the 2-D models were used as upper boundary conditions for the 1-D models.

OBJECTIVES:

1. Evaluate two-dimensional effects (such as bypass) on infiltration through the landfill cover. Previous modeling consisted of one-dimensional HELP models of the CWF and FWF.
2. Evaluate the effects of degradation of the cover including degradation of the clay barrier and clogging of the drainage layer.
3. Evaluate the effects of increased precipitation on model results.

SOLUTIONS/CONCLUSIONS/RESULTS:

- For the 2-D model base case flux upper boundary case (i.e., 0.145 in/yr), the average flux through the non-select fill is $\sim 6.05E-10$ cm/s.
- For the 2-D model increased flux upper boundary case (i.e., 1.245 in/yr), the average flux through the non-select fill is $\sim 3.72E-09$ cm/s.
- The 2-D model predicts an enhancement of vertical flux at the edges of the landfill due to the slope of the sand drainage layer and the performance cover.
- The base case 2-D model also predicts an average lateral flux from the claystone into the liner (below the cover) of $3.33E-11$ cm/sec on the SW side and $1.13E-11$ cm/sec on the NE side.

- The combination of (a) an increased clay liner conductivity due to cover degradation and (b) a lower horizontal conductivity of the sand drainage layer due to clogging results in predominantly vertical flow in the model domain.
- For the 1-D models, fluxes are increased by a scaling factor that takes into account increased flow due to sloping walls and flow diversion around waste canisters. The fluxes out of the models are approximately the same as the flux coming into the models.

MODELING:

2-DIMENSIONAL MODEL OF THE WASTE FACILITIES

The 2-D model was developed in response to a previous comment regarding effects (such as bypass) on infiltration through the cover. The model input/output files are attached.

Simulation Runs:

Two types of simulations were run for the 2-D model. The first set of simulations used a base case infiltration rate (0.145 in/yr) to represent current conditions and an increased infiltration rate (1.245 in/yr) to represent a future wetter climate for the area. The second type simulates the base case infiltration rate with the performance cover degraded and clogged conditions in the sand lateral drainage layer.

Model Domain and Setup:

The model geometry for the 2-D model was based on design specifications of the CWF. The model geometry is illustrated in Figure 1. For computational convenience, layers above the sand drainage layer were removed. The model extends from the top of the drainage layer (in the landfill) and the top of the OAG layer (in the undisturbed host medium) down to the elevation of the top of the reinforced shotcrete header positioned above the canister waste. The drainage layer has a thickness of 2 feet and the performance cover (top clay liner) has a thickness of 3 feet. Both of these layers have a 4% gradient sloping toward the OAG. At the edge of the landfill the performance cover and lateral clay liners merge, where the clay liner has an approximate thickness of 7.5 feet. Within the boundaries of the landfill, a layer of non-select red bed fill material is defined between the lower boundary of the model and the performance cover. The corresponding units outside the landfill are claystone and OAG.

Measured from the apex of the landfill, the southwest lateral boundary is 355 feet and the northeast boundary is 450 feet. The contact between the OAG and the claystone slopes away from the landfill in the lateral plane being modeled. To simulate the drainage, a seepage face boundary was specified (as per Scanlon et al., 2002) across the entire lower model boundary (the elevation of the reinforced shotcrete at the top of the waste). The lateral model boundaries were specified as no-flow boundaries. To emulate the flow of water along the OAG-claystone contact away from the waste, the OAG material

properties were applied vertically across the entire model over the last 50 feet of the model grid adjacent to the model lateral boundaries. This allowed water to exit the model based upon the seepage characteristics of the OAG without requiring an excessively large model grid.

Input:

VS2DI requires several parameters as input. Input parameters, such as soil parameters, initial conditions, and boundary conditions, are based on site descriptions, field investigations, lab results, design specifications, climate records, future climate predictions and conservative literature values.

2-D Simulations under Base case and Future Wetter Climate Infiltration Conditions

Saturated conductivity and porosity values were estimated or assigned to the various units based on actual measurements. The saturated conductivity for the performance cover is based on the RCRA liner and cover certification tests which averaged to approximately 4E-09 cm/s; Table 2 supplies the RCRA Liner/Cover Certification Tests (Cook-Joyce, Inc, 2004). The van Genuchten parameters defining the unsaturated characteristics are values from the literature for the components based on correspondence with soil texture and saturated conductivity. Table 1 provides these values along with the source.

Table 1: Hydrologic properties

Soil type	K_{sat} (cm/s)	Porosity (-)	VG α (1/cm)	VG n (-)	Source
OAG	3.5E-03	0.20	0.02	1.46	Scanlon et. all, 2002, Texas layer 3, Table 2
claystone	4.0E-09	0.29	0.0017	2.22	Table 6.6-4
redbed non select-fill	1.0E-06	0.15	0.0057	1.36	Benson et. all, 2004, Interim cover, Table 3
sand lateral drainage layer	1.0E-02	0.25	0.02	1.46	Scanlon et. all, 2002, Texas layer 3, Table 2
clay liner & performance cover	4.0E-09	0.30	0.0018	2.70	Cook-Joyce, Inc., 2004&2005

VS2DI does not include a module for modeling soil-atmosphere interactions at the top boundary; therefore, an analysis of the 1-D HELP model described in Appendix 8.0-6 was used to determine the net “ET-corrected” infiltration into the top of the 2-D model. The HELP model used an SCS curve number of 60 and two values of precipitation, 16 in/yr (base case) and 29 in/yr (future wetter climate), which resulted in base case infiltration and increased infiltration scenarios, respectively. 16 in/yr is the present-day average annual precipitation at the site, while the 29 in/yr (the climate record for Wichita, KS) was assumed to represent the wettest climate expected in the future over the period of analysis. The net infiltration for these two cases was computed by summing the drainage collected from the gravel bio layer (HELP model layer 4) and the infiltration into the moisture retention soil (HELP model layer 5) that lies above the sand lateral drainage layer. The resulting infiltrations for the 16 in/yr and 29 in/yr precipitation rates

topsoil, moisture retention soil, sand, gravel bio-barrier, non-select red bed, etc.) that provide additional protection. This multiple-layer system also minimizes the threat to the integrity of the performance cover from such aspects as freeze-thaw cycles, erosion, subsidence, root intrusion and animal intrusion.

The impact of initial flaws in clay barrier construction and shrink-swell cycles are being addressed by additional simulations. These simulations were carried out to investigate the impact of cover degradation and clogging of the sand drainage layer. As compared to the base case, this involved increasing the conductivity of the clay liner to $1\text{E-}8$ cm/s and decreasing the horizontal conductivity of the sand drainage layer from 0.01 cm/s to $1\text{E-}5$ cm/s (while the vertical conductivity was kept unchanged at 0.01 cm/s). These changes led to instability in the model which limited model runs to approximately 95 years. This time period was insufficient for the model to achieve steady state conditions. To reach steady state conditions, the OAG that was applied vertically over the last 50 ft of the model grid adjacent to the lateral model boundaries was redefined as claystone. Figure 2 shows the model geometry. This modification should be reasonable as there will be less flow to the OAG and more flow will enter through the cover. Initial conditions for the model were taken to be the same as the base case and increased flux upper boundary cases.

Results and Discussions:

2-D Simulations under Base Case and Future Wetter Climate Infiltration Conditions

Inter-layer and intra-layer vertical fluxes were computed at the center of the landfill and two locations on the flanks to quantify the nature of spatial variability in fluid flow behavior. Stable fluxes were obtained after $\sim 1\text{E}12$ seconds, and these results are summarized below.

For the base case flux upper boundary case (i.e., 0.145 in/yr), the flux into the performance cover at the apex is $\sim 2.2\text{E-}10$ cm/s, the flux from the performance cover to the non-select fill is $\sim 2.38\text{E-}10$ cm/s, and the flux through the non-select fill is $\sim 2.59\text{E-}10$ cm/s. The average flux across the landfill from the non-select fill into the shotcrete is approximately $6.05\text{E-}10$. This flux across the base of the non select fill is lower than the corresponding HELP result (i.e., $\sim 3\text{E-}9$ cm/s).

Fluxes at the edge of the landfill are higher than those along the apex. Table 3 provides the fluxes at the apex and the flanks at $\sim 1\text{E}12$ seconds. Flux ratios range from 3.2 to 3.7 along the longer (NE) flank and from 2.4 to 2.9 along the shorter (SW) flank.

The base case 2-D model also predicts an average lateral flux from the claystone into the liner (below the cover) of $\sim 3.33\text{E-}11$ cm/sec on the SW side and $\sim 1.13\text{E-}11$ cm/sec on the NE side.

Table 3: Inter-layer and Intra-layer fluxes at the apex and the two sides of the landfill for the simulation with the base case upper flux B.C.

	SW flank q (cm/s)	apex q (cm/s)	NE flank q (cm/s)
Sand Drainage Layer to Performance Cover	6.27E-10	2.20E-10	8.16E-10
Performance Cover to Non-Select Fill	6.25E-10	2.38E-10	7.97E-10
Through Non-Select Fill	6.26E-10	2.59E-10	8.18E-10

For the increased flux upper boundary case (i.e., 1.245 in/yr), the flux into the performance cover at the apex is $\sim 1.15\text{E-}09$ cm/s, the flux from the performance cover to the non-select fill is $\sim 1.26\text{E-}09$ cm/s, and the flux through the non-select fill is $\sim 1.44\text{E-}09$ cm/s. The average flux across the landfill from the non-select fill into the shotcrete is approximately $3.72\text{E-}09$. This computed flux into the waste is approximately the same as the corresponding HELP result (i.e., $\sim 4\text{E-}9$ cm/s).

The flux at locations close to the edge of the landfill along the longer (NE) flank and the shorter (SW) flank are both higher than along the apex. Computed values of flux at the apex and the flanks after $1\text{E}12$ seconds are given in Table 4. Along the longer flank, the flux ratios range from 3.5 to 4.4; and along the shorter flank, the flux ratios range from 2.7 to 3.4.

Table 4: Inter-layer and Intra-layer fluxes at the apex and the two sides of the landfill for the simulation with an increased upper flux B.C.

	SW flank q (cm/s)	apex q (cm/s)	NE flank q (cm/s)
Sand Drainage Layer to Performance Cover	3.88E-09	1.15E-09	5.04E-09
Performance Cover to Non-Select Fill	3.87E-09	1.26E-09	4.93E-09
Through Non-Select Fill	3.88E-09	1.44E-09	5.09E-09

Although the current model was developed based on the geometry for the CWF, its general conclusions with respect to flux enhancement at the edges should also be valid for the FWF. As a matter of comparison, the two sloping flanks for the FWF are 189 ft and 655 ft as compared to 170 ft and 280 ft for the CWF.

In summary, the 2-D model predicts an enhancement of vertical flux at the edges of the landfill due to the slope of the sand drainage layer and the performance cover. However, the base case flux calculated by rigorously solving Richards' equation for 2-D unsaturated flow is found to be significantly lower than the flux predicted by the simpler base case HELP model (which assumes unit gradient drainage under fully saturated conditions). Thus, for the base case, results from the HELP model represent a conservative upper bound for the flux into the waste.

2-d Simulations with Cover Degradation

Inter-layer and intra-layer vertical fluxes were computed at the same locations as the models without degradation and clogging. Stable fluxes were obtained after $\sim 1E12$ seconds.

Decreasing the horizontal conductivity of the sand drainage layer reduces lateral migration of water and creates more uniform flux distribution along the entire length of the drainage layer. The vertical flux from the drainage layer into the performance cover is increased by a factor of ~ 40 to $\sim 8.80E-09$ cm/s at the apex. The fluxes along the flanks are similar to this value, as is seen in Table 5, because the flow pattern has become predominantly vertical due to the increased anisotropy ratio. In other words, there is less enhancement of vertical flux along the edges. The average flux across the landfill from the non-select fill into the shotcrete is approximately $1.21E-08$.

Table 5: Inter-layer and intra-layer fluxes at the apex and two sides of the landfill for simulation with degradation of the clay liner and clogging in the sand drainage layer.

	SW flank	apex	NE flank
	q (cm/s)	q (cm/s)	q (cm/s)
Sand Drainage Layer to Performance Cover	1.17E-08	8.80E-09	1.16E-08
Performance Cover to Non-Select Fill	1.17E-08	9.46E-09	1.14E-08
Through Non-Select Fill	1.17E-08	9.96E-09	1.17E-08

The flux from the performance cover into the non-select fill increased by a factor of ~ 40 to $\sim 9.46E-09$ cm/sec at the apex. As before, the fluxes along the flanks are similar to that at the apex – indicating a predominantly vertical flow system. Some lateral flow within the sand drainage layer and the top of the clay liner still occurs because the throughput potential (i.e., saturated conductivity) of the clay liner is several orders of magnitude lower than that of the sand drainage layer. The flux through the non-select fill has increased by a factor of ~ 38 to $\sim 9.96E-09$ cm/s.

In summary, the combination of (a) an increased clay liner conductivity due to cover degradation and (b) lower horizontal conductivity of the sand drainage layer due to clogging results in predominantly vertical flow in the model domain. This minimizes spatial variability of vertical flux, and also enhances the magnitude of the downward flux.

1-DIMENSIONAL MODEL OF WASTE AREA

Simulation Runs:

1-D models were developed for each of the waste areas: the FWF section with bulk waste, the FWF section with canister waste, and the CWF with canister waste. For each

of these three areas, three simulations were run assuming dimensions and a flow pattern that are representative of flow through the apex and the SW and NE flanks of the waste facilities. Upper boundary fluxes were based on the model output of the 2-D simulations for base case precipitation, future wetter climate precipitation, and base case precipitation with a degraded landfill cover. Simulations based on average flux across the 2-D models were also performed for each of the waste areas using the apex model dimensions. Additional runs were developed to simulate infiltration through the waste areas excluding the landfill cover. These simulations are designed to be representative of the operational period when the waste facilities will be without the landfill cover (cap) and exposed to the elements.

Model Domain and Setup:

1-D model of waste sites with cover

The model geometry for the 1-D models through the waste areas extends from the bottom of the redbed non-select fill to the base of the waste site. The CWF and FWF canister waste models contain a 1.5 feet thick slab of reinforced shotcrete, which is underlain by a sand column. The sand columns represent the sand that will be inserted between the canisters. The FWF bulk waste model also contains a 1.5 feet thick slab of reinforced shotcrete, but is underlain with bulk waste.

1-D model of waste sites without cover

The model geometry for the 1-D models without a cover is identical to the 1-D models with the cover except that the reinforced shotcrete was removed.

Input:

VS2DI requires several parameters as input. Input parameters, such as soil parameters, initial conditions, and boundary conditions, are based on site descriptions, field investigations, lab results, design specifications, climate records, future climate predictions and conservative literature values.

1-D model of waste sites with cover

Saturated conductivity and porosity values were estimated or assigned to the various units based on actual measurements. The van Genuchten parameters defining the unsaturated characteristics are values from the literature for the components based on correspondence with soil texture and saturated conductivity. The bulk waste is assumed to have the properties of sand, albeit with a lower K_{sat} . Table 6 provides these values along with the source.

Table 6: Hydrologic Properties for 1-D model

Soil type	K_{sat} (cm/s)	Porosity (-)	VG α (1/cm)	VG n (-)	Source
Bulk Waste	1.0E-04	0.25	0.02	1.46	Scanlon et. all, 2002, Texas layer 3, Table 2
Sand	1.0E-02	0.25	0.02	1.46	Scanlon et. all, 2002, Texas layer 3, Table 2.
Reinforced Shotcrete Header	5.0E-07	0.30	0.0018	2.70	

The upper boundary conditions assume fluxes through the redbed non-select fill as calculated by the 2-D models. These fluxes are increased by a scaling factor that takes into account increased flow due to sloping walls and flow diversion around waste canisters. The scaling factors for the three modeling sites are listed in Table 7 and the corresponding upper boundary fluxes are listed in Table 8. The scaling factors for the canister waste sites are large compared to the bulk waste site because they scale to flow between the canisters. However, the yearly yield per square meter flowing out at the bottom of the landfills will be similar in magnitude.

Initial soil moisture content in the layers was defined at 0.1 for all soil types.

Table 7: Upscaling factors to account for increased flow at the bottom of the model

Model	Scale-factor
FWF with bulk waste	1.245
FWF with canister waste	5.79
CWF with canister waste	5.32

Table 8: Upper boundary fluxes for various models

Modeling case	Upper BC	SW flank q (cm/s)	Apex q (cm/s)	NE flank q (cm/s)	Average q (cm/s)
FWF bulk waste	Base case flux	7.79E-10	3.22E-10	1.02E-09	7.53E-10
FWF canister waste	Base case flux	3.62E-09	1.50E-09	4.74E-09	3.50E-09
CWF	Base case flux	3.33E-09	1.38E-09	4.35E-09	3.22E-09
FWF bulk waste	Future wetter climate flux	4.83E-09	1.80E-09	6.34E-09	4.64E-09
FWF canister waste	Future wetter climate flux	2.25E-08	8.36E-09	2.95E-08	2.16E-08
CWF	Future wetter climate flux	2.06E-08	7.68E-09	2.71E-08	1.98E-08
FWF bulk waste	Degradation flux	1.46E-08	1.24E-08	1.46E-08	1.51E-08
FWF canister waste	Degradation flux	6.79E-08	5.77E-08	6.77E-08	7.02E-08
CWF	Degradation flux	6.24E-08	5.30E-08	6.22E-08	6.45E-08

1-D model of waste sites without cover

As mentioned earlier, the reinforced shotcrete is removed for the operational period models. The waste facilities without the landfill cover will have infiltration approximately equal to the precipitation. The three models were run considering the base precipitation of 16 in/yr and an increased precipitation of 29 in/yr. The two input fluxes are scaled using the up scaling-factors given in Table 7.

Results and Discussions:

1-D model of waste sites with cover

Fluxes were computed at the bottom of the columns. Stable fluxes were obtained after approximately 1E11 seconds, and are summarized below.

For the base case flux upper boundary, the average flux at the bottom of the waste sites is $\sim 3.22\text{E-}09$ cm/s, $\sim 3.46\text{E-}09$ cm/s, $\sim 7.47\text{E-}10$ cm/s for the CWF canister waste site, the FWF canister waste site and the FWF bulk waste site, respectively. The flux at locations close to the edge of the landfill along the longer (NE) flank and the shorter (SW) flank are both higher than along the apex (Table 9). Along the longer flank, the flux ratio is ~ 3.2 for all three sites; and along the shorter flank, the flux is ~ 2.4 .

The average leakage is estimated by multiplying the average bottom calculated flux by the bottom area open to flow (excluding the area occupied by waste canisters). The estimated leakage for the CWF canister waste site, the FWF canister waste site and the FWF bulk waste site is approximately $6.41\text{E-}07$ $\text{m}^3 / \text{day} \cdot \text{m}^2$, $6.66\text{E-}07$ $\text{m}^3 / \text{day} \cdot \text{m}^2$, and $6.45\text{E-}07$ $\text{m}^3 / \text{day} \cdot \text{m}^2$, respectively.

Table 9: Fluxes at the base of the 1-D models with a base case flux upper B.C.

	SW flank q (cm/s)	Apex q (cm/s)	NE flank q (cm/s)	Average q (cm/s)
CWF	3.32E-09	1.38E-09	4.34E-09	3.22E-09
FWF canister waste	3.62E-09	1.49E-09	4.69E-09	3.46E-09
FWF bulk waste	7.77E-10	3.20E-10	1.01E-09	7.47E-10

For the future wetter climate flux upper boundary, the average flux at the bottom of the waste sites is $\sim 1.98\text{E-}08$ cm/s, $\sim 2.14\text{E-}08$ cm/s, $\sim 4.59\text{E-}09$ cm/s for the CWF canister waste site, the FWF canister waste site and the FWF bulk waste site, respectively. The flux at locations close to the edge of the landfill along the longer (NE) flank and the shorter (SW) flank are both higher than along the apex (Table 10). Along the longer flank, the flux ratio is ~ 3.5 for all three sites; along the shorter flank, the flux ratio is ~ 2.7 . The average estimated leakage for the CWF canister waste site, the FWF canister waste site and the FWF bulk waste site is approximately $3.94\text{E-}06$ $\text{m}^3 / \text{day} \cdot \text{m}^2$, $4.12\text{E-}06$ $\text{m}^3 / \text{day} \cdot \text{m}^2$, and $3.97\text{E-}06$ $\text{m}^3 / \text{day} \cdot \text{m}^2$, respectively.

Table 10: Fluxes at the base of the 1-D models with a future wetter climate flux upper B.C.

	SW flank q (cm/s)	Apex q (cm/s)	NE flank q(cm/s)	Average q (cm/s)
CWF	2.06E-08	7.66E-09	2.70E-08	1.98E-08
FWF canister waste	2.25E-08	8.27E-09	2.92E-08	2.14E-08
FWF bulk waste	4.82E-09	1.78E-09	6.28E-09	4.59E-09

For the cover degradation flux upper boundary case, the average flux at the bottom of the waste sites is $\sim 6.45\text{E-}08$ cm/s, $\sim 6.95\text{E-}08$ cm/s, $\sim 1.50\text{E-}08$ cm/s for the CWF canister waste site, the FWF canister waste site and the FWF bulk waste site, respectively. The flux at locations close to the edge of the landfill along the longer (NE) flank and the shorter (SW) flank are only slightly higher than along the apex (Table 11). The average estimated leakage for the CWF canister waste site, the FWF canister waste site and the FWF bulk waste site is approximately $1.28\text{E-}05$ $m^3 / day \cdot m^2$, $1.34\text{E-}05$ $m^3 / day \cdot m^2$, and $1.3\text{E-}05$ $m^3 / day \cdot m^2$, respectively.

Table 11: Fluxes at the base of the 1-D models with upper flux B.C obtained from flow through the redbed non-select fill of the 2-D model with degradation.

	SW flank q (cm/s)	Apex q (cm/s)	NE flank q (cm/s)	Average q (cm/s)
CWF	6.22E-08	5.28E-08	6.22E-08	6.45E-08
FWF canister waste	6.79E-08	5.71E-08	6.70E-08	6.95E-08
FWF bulk waste	1.46E-08	1.23E-08	1.45E-08	1.50E-08

1-D model of waste sites without cover

Fluxes were computed at the bottom of the columns after simulations were terminated at $\sim 1\text{E}10$ seconds upon the attainment of stable (quasi-steady) vertical fluxes, and these results are summarized below.

For the 16 in/yr ($1.29\text{E-}06$ cm/sec) case, the estimated leakage for the CWF canister waste site, the FWF canister waste site and the FWF bulk waste site is approximately $1.36\text{E-}03$ $m^3 / day \cdot m^2$, $1.42\text{E-}03$ $m^3 / day \cdot m^2$, and $1.37\text{E-}03$ $m^3 / day \cdot m^2$, respectively. For the 29 in/yr ($2.34\text{E-}06$ cm/sec) case, the estimated leakage for the CWF canister waste site, the FWF canister waste site and the FWF bulk waste site is approximately $2.47\text{E-}03$ $m^3 / day \cdot m^2$, $2.58\text{E-}03$ $m^3 / day \cdot m^2$, and $2.49\text{E-}03$ $m^3 / day \cdot m^2$, respectively.

Table 12: Fluxes without the cover at the base of the 1-D models.

	q (cm/s) for 16 in/yr case	q (cm/s) for 29 in/yr case
CWF	6.84E-06	1.24E-05
FWF canister waste	7.38E-06	1.34E-05
FWF bulk waste	1.59E-06	2.88E-06

Derivation of Scaling Factors:

The walls of the FWF and the CWF are sloped resulting in more area available for flow at the top than at the bottom. This will result in increased flow towards the bottom. In order to model a unit area of the waste that accounts for the increased flow at the bottom, the top flow has to be scaled by the area open to flow at the top of the waste divided by the area open to flow at the bottom of the model.

The FWF section with bulk waste is assumed to have uniform hydraulic properties. The resulting the flow for the FWF section with bulk waste, q_{bulk} , will be

$$q_{bulk} = \frac{w_{top}}{w_{bottom}} q_{top},$$

with w_{top} and w_{bottom} as the top and bottom width of the FWF.

The fluxes at the CWF and the FWF section with canister waste have to account for space taken up by the canisters. Canisters are stacked directly on top of each other and are spaced approximately 12 inches from one another in each row. Each new row has 4 more canisters than the row below it. Figure 3 gives a cross-sectional schematic of the canister positions. The FWF will have 110 canisters in the bottom row and 134 canisters in the top row. The CWF will have 62 and 72 canisters in the bottom and top rows respectively.

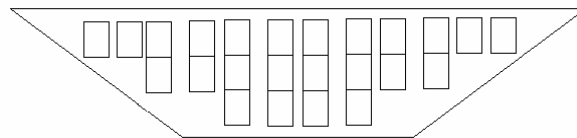


Figure 3: Schematic cross-section displaying positioning of canisters in the waste facilities

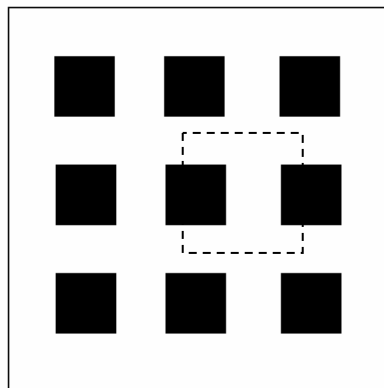


Figure 4: Schematic of top view of canister positioning at the waste facilities

From the schematic of the aerial view of canister positioning at the waste facilities (Figure 4), one can see that in front and behind canisters there is additional area open to flow. To account for this, the area open to flow at the bottom of the waste facilities with canister waste will be the cross-sectional width times the width of the canister and twelve inches for the separation between canisters minus the top-area of all the canisters at the bottom. The area open to flow at the top of the waste facilities with canister waste will be the cross-sectional width times the width of the canister and twelve inches for the separation between canisters. Note that the top area does not account for canister waste, because flow enters over the entire top area. This results in the following scaled flow at the top of the CWF and FWF site with canister waste.

$$q_{\text{CWFcanister}} = \frac{(w_{12} + w_{\text{can}})w_{\text{top}}}{(w_{12} + w_{\text{can}})w_{\text{bottom}} - 62A_{\text{can}}} q_{\text{top}}$$

$$q_{\text{FWFcanister}} = \frac{(w_{12} + w_{\text{can}})w_{\text{top}}}{(w_{12} + w_{\text{can}})w_{\text{bottom}} - 110A_{\text{can}}} q_{\text{top}}$$

with w_{top} and w_{bottom} as the top and bottom width of the landfills and with w_{12} , w_{can} , and A_{can} as the width of the space between canisters, the canister width, and the area of the top of the canister, respectively.

References

Benson, C.H., G.L. Bohnhoff, P. Apinwantragoon, A.S. Ogorzalek, C.D. Shackelford and W.H. Albright, 2004, "Comparisons of model predictions and field data for an ET cover", Proc., Tailings and Mine Waste '04, pp. 137-142.

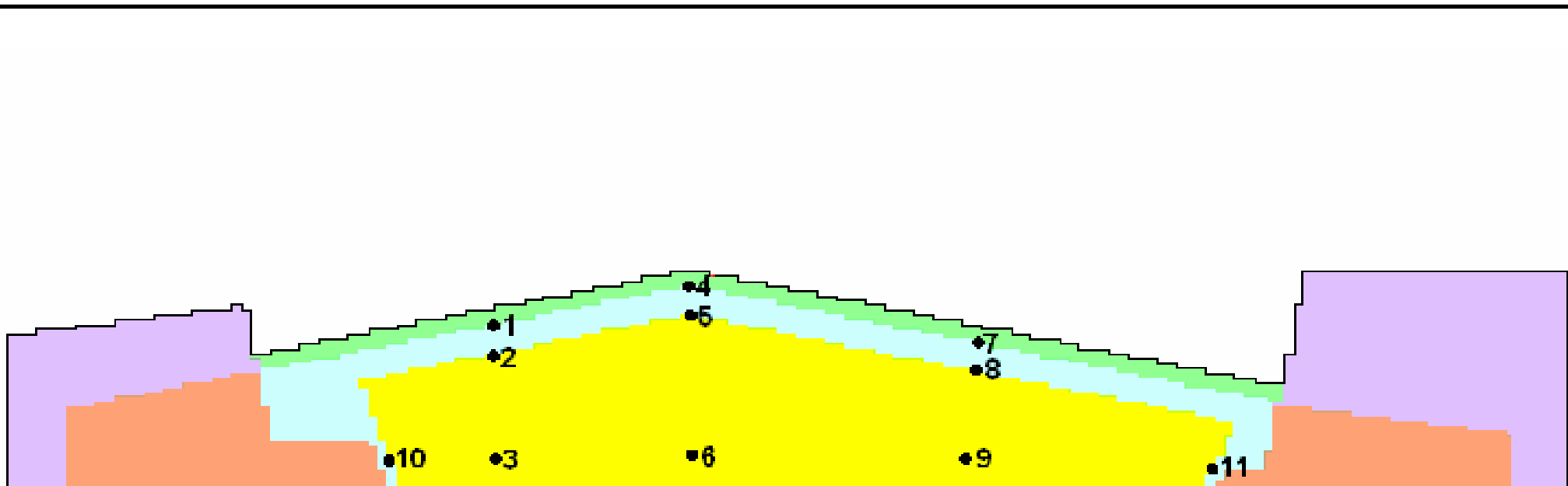
Cook-Joyce, Inc., Dec 2004, "the East+West landfill Cells A and B Final Cover Construction Certification Report", TCEQ Permit No. HW-50358. Prepared for Waste Control Specialists LLC.

Cook-Joyce, Inc., Mar 2005, "the East+West landfill Cells F and G liner Construction Certification Report", TCEQ Permit No. HW-50358. Prepared for Waste Control Specialists LLC.

Hsieh, P.A., Wingle, William, and Healy, R.W., 1999, VS2DI--a graphical software package for simulating fluid flow and solute or energy transport in variably saturated porous media: U.S. Geological Survey Water-Resources Investigations Report 99-4130, 16 p.

Scanlon, B.R., M. Christman, R.C. Reedy, I. Porro, J. Simunek and G.N. Flerchinger, 2002, "Intercode comparisons for simulating water balance of surficial sediments in semiarid regions", Water Resources Res., Vol. 38(12), 1323.

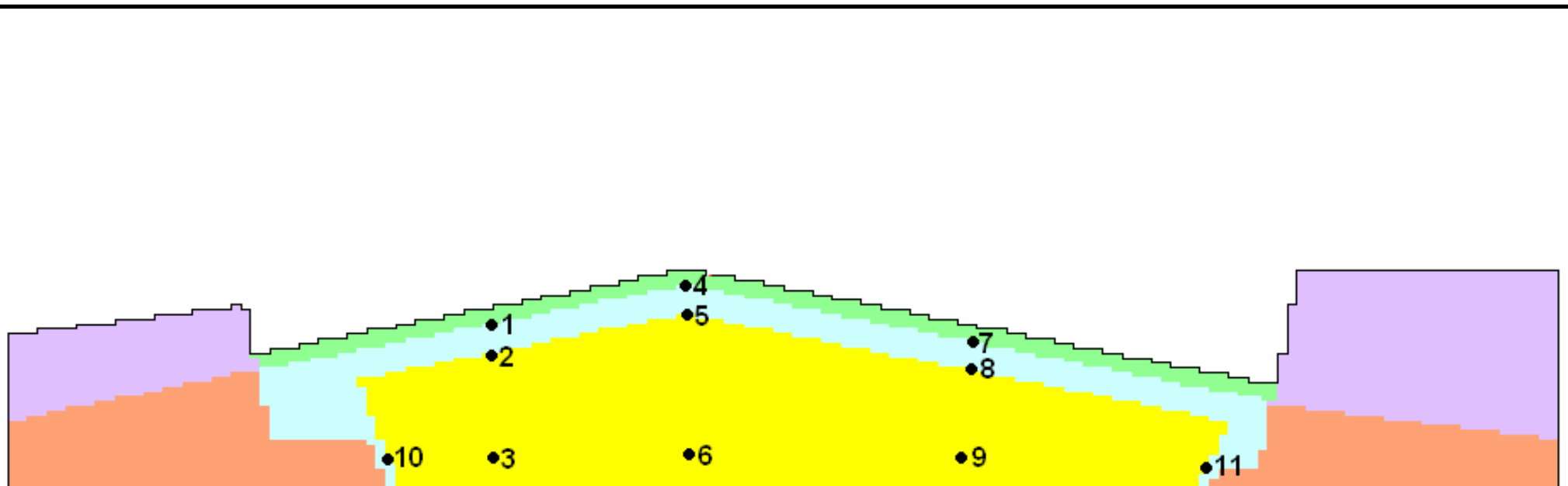
Suter, G.W. II, Luxmoore, R.J., Smith, E.D., 1993, "Compacted soil barriers at abandoned landfill sites are likely to fail in the long term", Journal of Environmental Quality. Vol 22 no 2.








Color	Name
purple	OAG
orange	mudstone
green	sand lateral drainage
light blue	performance cover
yellow	redbed non-select fill

Model schematic and locations of calculated fluxes for the 2-D models with a base case flux upper B.C. and increased flux upper B.C.

Figure 1



Color	Name
	OAG
	mudstone
	sand lateral drainage
	performance cover
	redbed non-select fill

Model schematic and locations of calculated fluxes for the 2-D models with a degraded cover.

Figure 2

ATTACHMENT 1

Spread of Water beneath a Leaking Concrete Landfill Cover

Robert M. Holt
Department of Geology and Geological Engineering
University of Mississippi
662-915-6687
rmholt@olemiss.edu

Here we develop a simple analytical approach for determining the lateral spread of water in landfill sediments beneath a leaking concrete cover at the WCS landfill. The landfill is subdivided into twenty five 100 ft \times 1,500 ft cells, each with a separate drain system. The thickness of landfill sediments is 24 m. The primary objective is to determine if the location of a leak through the concrete cover can be identified by sampling flow rates within the drains of each cell.

Since the lateral spread of water is maximized at steady state, we assume that flow within in the landfill is governed by the steady-state form of Richards' equation

$$\nabla \cdot [K(\psi) \nabla \psi] = \frac{\partial K(\psi)}{\partial z}, \quad (1)$$

where ψ is the matric potential, $K(\psi)$ is the unsaturated hydraulic conductivity, and z is the vertical ordinate oriented positively downward. Equation (1) is non-linear and difficult to solve analytically. However, the quasilinear form of Richards' equation is quite amenable to analytical solutions

$$\nabla^2 \Theta = \alpha \frac{\partial \Theta}{\partial z}, \quad (2)$$

where Θ is the matric flux potential and α is a soil parameter related to the inverse of the macroscopic capillary length scale of Philip (1984). The matric flux potential is given by

$$\Theta = \int_{\psi_i}^{\psi} K(\psi) d\psi, \quad (3)$$

where ψ_i is the initial matric potential in the soil, and the macroscopic capillary length can be determined for any arbitrary $K(\psi)$ using

$$\lambda_c = \alpha^{-1} = \frac{1}{K(\psi_0) - K(\psi_i)} \int_{\psi_i}^{\psi_0} K(\psi) d\psi, \quad (4)$$

where ψ_0 is the maximum matric potential in the domain. Using an exponential unsaturated hydraulic conductivity model, equation (2) becomes exact, e.g.,

$$K(\psi) = K_s e^{\alpha\psi}, \quad (5)$$

where K_s is the saturated hydraulic conductivity. When equation (4) is used to calculate α from an arbitrary $K(\psi)$, equation (2) is correct in an integral sense (Philip, 1985). While reported ranges of α vary from $\sim 0.001 \text{ cm}^{-1}$ to 1 cm^{-1} , α in most soils ranges from 0.01 cm^{-1} to 0.1 cm^{-1} .

We assume that the leak through the concrete cap is limited to a single point and that the landfill cap is otherwise impermeable to water. This allows us to consider the leak a point source and prescribe a no-flow upper boundary condition similar to that of the land surface. Because the lateral dimensions of the landfill are large ($1,500 \text{ ft} \times 2,500 \text{ ft}$) relative to the macroscopic capillary length of most soils, we assume that the soil has an infinite areal extent. Because the landfill is relatively thick, we neglect the lower boundary condition and assume that the soil has an infinite depth. This assumption is conservative, likely leading to greater spreading. Quasilinear solutions for buried point sources in the presence of a water table show that the water table concentrates the flow towards the region vertically beneath the source (Philip, 1989). Drains at the base of the landfill will achieve a similar result. This conceptualization is consistent with a quasilinear analytical solution developed by Raats (1971) for surface point sources in homogenous medium of infinite depth.

Raats (1971) developed an analytical solution for a surface point source using a non-dimensional form of equation (2)

$$\frac{1}{R} \frac{\partial}{\partial R} \left(R \frac{\partial v}{\partial R} \right) + \frac{\partial^2 v}{\partial Z^2} = 2 \frac{\partial v}{\partial Z}, \quad (6)$$

where R is the dimensionless radial coordinate, Z is the dimensionless vertical coordinate, and v is the dimensionless matric flux potential. Here dimensionless space coordinates are related to their dimensional counterparts by

$$\frac{R}{r} = \frac{Z}{z} = \frac{\alpha}{2}, \quad (7)$$

and v is the dimensionless matric potential defined by

$$v = \frac{8\pi\Theta}{\alpha Q}, \quad (8)$$

where Q is the volumetric discharge at the point source. Raats (1971) solved equation (6) with a source singularity of strength 2π at the origin and boundary conditions of no flow through the surface ($Z = 0, 0 < R \leq \infty$) and $v = 0$ at $R = \infty$ and $Z = \infty$. His analytical solution is

$$v = 2 \left\{ \frac{e^{Z-T}}{T} + e^{2Z} \text{Ei}[-(Z+T)] \right\}, \quad (9)$$

where Ei is the exponential integral and $T = (R^2 + Z^2)^{1/2}$. The associated dimensionless Stokes stream function is (Raats, 1971)

$$\Psi_D = \frac{Z}{T} e^{Z-T}. \quad (10)$$

The dimensional stream function can be determined using $\Psi = \Psi_D Q$.

Because two stream functions define a stream tube and the volumetric discharge of the stream tube is simply the difference between the two stream functions, we can use equation (10) to determine the fraction of the total discharge at the source (Q) captured by a circular area centered directly below the source at any arbitrary depth. This fraction is defined by

$$f = 1 - \Psi_D(Z_1, R_1). \quad (11)$$

where Z_1 is a dimensionless depth (e.g., the depth to the landfill liner at 24 m) and R_1 is the dimensionless radius of the circular area. Note that $\Psi_D(Z_1, \infty) = 0$. It is important to recognize that specific solutions for f only depend on α , which scales the space coordinates, and does not depend on other soil hydraulic properties (e.g., hydraulic conductivity, porosity, etc.).

Plots of f (evaluated at a depth of 24 m) versus dimensional radius (Figure 1) show that for most soils ($0.01 \text{ cm}^{-1} \leq \alpha \leq 1 \text{ cm}^{-1}$) over 80% of the discharge from a leak in the concrete

landfill cover will be captured within a circular area with a 40 ft radius. Unless the cover leak is fairly close to a cell boundary, it should be possible to narrow down the leak location to a single cell.

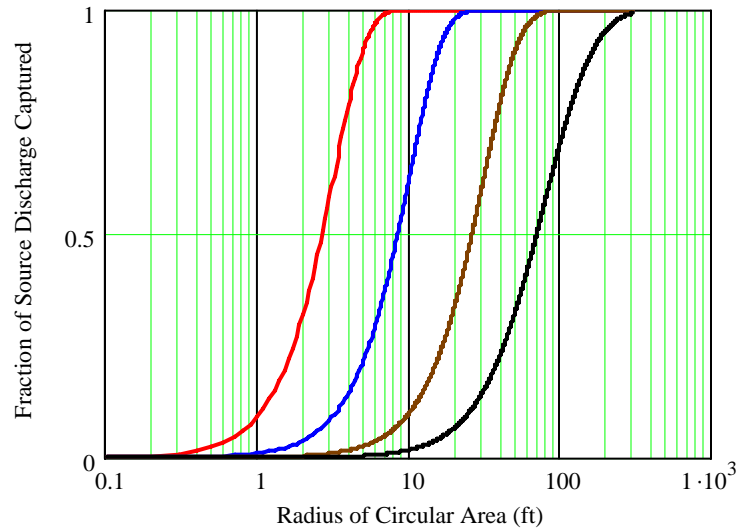


Figure 1. Fraction of the total source discharge captured by a circular area centered directly below the source at 24 m depth, for α equal to 1.0 cm^{-1} (red), 0.1 cm^{-1} (blue), 0.01 cm^{-1} (brown), and 0.001 cm^{-1} (black).

References

- Philip, J. R., 1984, Aspects of quasilinear infiltration from surface sources, especially the case $\alpha = 0$, *Water Resources Research*, Vol. 20, p. 633-635.
- Philip, J. R., 1985, Reply to "Comments on steady infiltration from spherical cavities," *Soil Science Society of America Journal*, Vol. 49, p. 788-789.
- Philip, J. R., 1989, Multidimensional steady infiltration to a water table, *Water Resources Research*, Vol. 25, p. 109-116.
- Ratts, P. A. C., 1971, Steady infiltration from point sources, cavities and basins, *Soil Science Society of America Journal*, Vol. 35, p. 689-694.

Appendix A
Mathcad 2001 Worksheet for Calculating the Dimensionless Fraction
of Flux Captured by a Circular Area

Spread of Water beneath a Leaking Concrete Cap

Define the dimensionless buried point source solution and surface source solution:

$$\Theta_b(Z, R) := \frac{e^{-Z \cdot (R^2 + Z^2)^{0.5}}}{(R^2 + Z^2)^{0.5}}$$

Define the dimensionless stream lines:

$$\Psi_s(Z, R) := Z \cdot \Theta_b(Z, R)$$

Specify depth to base of landfill

$$z_1 := 24 \cdot 100 \quad \text{cm}$$

Define the dimensionless depth of observation:

$$Z_1(\alpha) := \frac{\alpha \cdot z_1}{2}$$

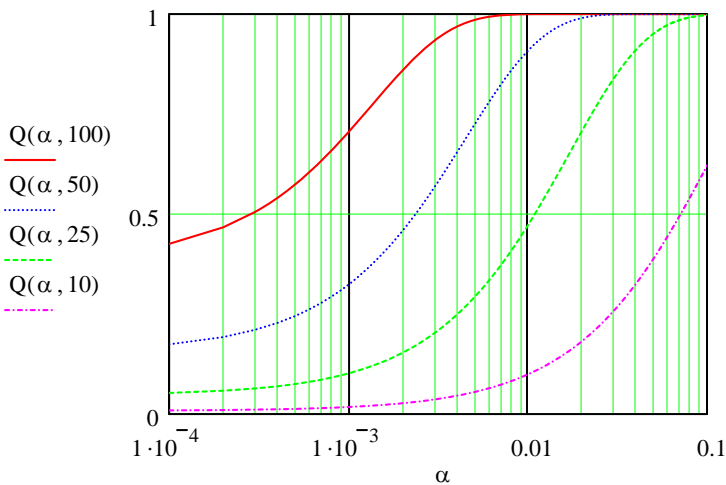
Function for converting feet to cm:

$$f(r) := r \cdot 0.3048 \cdot 100$$

Function to estimate the total fraction of the flux passing through a dimensionless radius of $\alpha/2$:

$$Q(\alpha, r) := 1 - \Psi_s\left(Z_1(\alpha), f(r) \cdot \frac{\alpha}{2}\right) \quad \alpha := 0.0001, 0.0002 \dots 0.1$$

Fraction of flux captured with a radius of 100, 50, 25, and 10 ft



$r := 0.1, .2 \dots 300$

Fraction of the total source discharge captured by a circular area centered directly below the source at 24 m depth, for α equal to 1.0 cm^{-1} (red), 0.1 cm^{-1} (blue), 0.01 cm^{-1} (brown), and 0.001 cm^{-1} (black).

